

Spin-Hall interface resistance in terms of Landauer-type spin dipoles

A. G. Mal'shukov,¹ L. Y. Wang,² and C. S. Chu²

¹*Institute of Spectroscopy, Russian Academy of Science, 142190 Troitsk, Moscow oblast, Russia*

²*Department of Electrophysics, National Chiao Tung University, Hsinchu 30010, Taiwan*

(Received 9 November 2006; published 12 February 2007)

We considered the nonequilibrium spin dipoles induced around spin-independent elastic scatterers by the intrinsic spin-Hall effect associated with the Rashba spin-orbit coupling. The spin polarization normal to the two-dimensional electron gas (2DEG) has been calculated in the diffusion range around the scatterer. Although around each impurity this polarization is finite, we found that the corresponding macroscopic spin density obtained via averaging of individual spin dipole distributions over impurity positions is zero in the bulk. At the same time, the spin density is finite near the boundary of 2DEG, except for a special case of a hard wall boundary, that is, when it turns to 0. The boundary value of the spin polarization can be associated with the interface spin-Hall resistance determining the additional energy dissipation due to spin accumulation.

DOI: [10.1103/PhysRevB.75.085315](https://doi.org/10.1103/PhysRevB.75.085315)

PACS number(s): 73.40.Lq, 72.25.Dc, 71.70.Ej

I. INTRODUCTION

Most of the theoretical studies on the spin-Hall effect (SHE) have been devoted to the calculation of the spin current (for a review, see Ref. 1). Such a current is a linear response to the external electric field \mathbf{E} , which induces a spin flux of electrons or holes flowing in the direction perpendicular to \mathbf{E} . This spin flux can be due either to the intrinsic spin-orbit interaction (SOI) inherent to a crystalline solid² or to the spin-dependent scattering from impurities.³ The spin-Hall current, as a response to the electric field, is characterized by the spin-Hall conductivity. On the other hand, similar to the conventional Hall effect, one can introduce the spin-Hall resistivity to the calculation of the local chemical potential difference $\mu_s = \mu_\uparrow - \mu_\downarrow$ as a response to the dc electric current. For the two-dimensional electron gas (2DEG) in a local equilibrium, this potential difference can be related to the z -component (perpendicular to 2DEG) of the spin polarization according to $S_z = N_F \mu_s$, where N_F is the density of states near the Fermi level. Therefore, the spin-Hall resistivity is closely associated with spin accumulation near the interfaces. It should be noted that measuring spin polarization is thus far the only realistic way to detect SHE.^{4,5} For interfaces of various types, such an accumulation has been calculated in a number of works.⁶⁻¹² A typical example to study spin accumulation is an infinite 2D strip along the x -direction with a width w along the y -direction. In this geometry, the dc flows in the x -direction while the spin-Hall current flows in the y -direction, with the spin density accumulating near the boundaries. An analog of the Hall voltage could be a difference of μ_s on both sides of the strip. There is, however, a fundamental distinction from the charge Hall effect. In the latter case, due to the long-range nature of the electric potential created by conserving electric charges, the Hall voltage is proportional to the width of the strip. In contrast, the spin-Hall electrochemical potential at the interface does not depend on w as $w \rightarrow \infty$ because spin relaxation essentially suppresses the long-range contribution to spin-polarization buildup near the interfaces. Hence, it is sensible to introduce an interface spin-Hall resistance, which is the proportionality coefficient between the interface value of μ_s and the electric current density.

Below, we will consider the spin-Hall resistance from the microscopic point of view. This approach is based on

Landauer's¹³ idea that at a given electric current, each impurity is surrounded by a nonequilibrium charge cloud forming a dipole. Combined together, these dipoles create a voltage drop across the sample. Therefore, each impurity plays a role of an elementary resistor. In a similar way, nonequilibrium spin dipoles could be induced subsequent to the spin-Hall current. One may expect that the spin cloud will appear around a spin-orbit scatterer in the case of an extrinsic SHE, as well as around a spin-independent scatterer in the case of the intrinsic effect. The latter possibility for a 2D electron gas with Rashba interaction has been considered in Ref. 14. The polarization perpendicular to 2DEG was calculated within the ballistic range around a scatterer. On the other hand, in order to study spin accumulation and the spin-Hall resistance on a macroscopic scale, one needs to calculate the spin-density distribution at distances much larger than the mean free path l of electrons. Below, we will extend the Green's function method of Ref. 14 to the diffusive range. In Sec. II, the spin-density distribution around an individual target impurity will be calculated. In Sec. III, we will consider the interface spin accumulation created by spin dipoles randomly but homogeneously distributed in space. A relation between spin-Hall resistance and energy dissipation will be discussed in Sec. IV. A summary and discussion of results will be presented in Sec. V.

II. SPIN CLOUD INDUCED BY A SINGLE IMPURITY

It is known that the electric field applied to a homogeneous 2DEG with the Rashba SOI induces a component of the nonequilibrium spin polarization parallel to 2DEG.¹⁵ The spin-Hall effect produces, however, a zero-spin polarization in its z -component. This understanding about such a *homogeneous* gas has implied an averaging over impurity positions. An impure system, on the other hand, cannot be uniform on a microscopic scale. The effect of each impurity on the spin polarization could be singled out by considering an impurity (a target impurity) at a fixed position while taking at the same time the average over positions of other impurities. In such a way, the Landauer electric dipole has been calculated.^{16,17} The electron density around a target impurity represented by the elastic scatterer was found from the

asymptotic expansion of the scattered wave functions of the electrons. At the same time, the wave vectors of incident particles were weighted with the nonequilibrium part of the Boltzmann distribution function. We will employ another method based on the Green's function formalism.¹⁴ Within this method, the spin-density response to the electric field \mathbf{E} is given by the standard Kubo formula, with the scattering potential of the target impurity incorporated into the retarded and advanced Green's functions $G^{r/a}(\mathbf{r}, \mathbf{r}', \omega)$ denoted by the superscripts r and a , respectively. As such, the n -component of the stationary spin polarization is given by

$$S_n(\mathbf{r}) = -\frac{e}{m^*} \int d^2 r' \int \frac{d\omega}{2\pi} \frac{dn_F(\omega)}{d\omega} \times \overline{\text{Tr}[\sigma^n G^r(\mathbf{r}, \mathbf{r}', \omega)(\mathbf{v}\mathbf{E})G^a(\mathbf{r}', \mathbf{r}, \omega)]}, \quad (1)$$

where the overbar denotes averaging over impurity positions, the trace runs through the spin variables, and $n_F(\omega)$ is the Fermi distribution function. To avoid further confusion, we note that the angular momentum is obtained by multiplying $S_n(\mathbf{r})$ by $\hbar/2$ and e is the particle charge, which is negative for electrons. At low temperatures, only ω in close vicinity around E_F contributes to the integral in Eq. (1). Therefore, below we set $\omega = E_F$ and omit the frequency argument in Green's functions. Further, \mathbf{v} is the particle velocity operator containing a spin-dependent part associated with SOI. Writing SOI in the form

$$H_{\text{so}} = \mathbf{h}_{\mathbf{k}} \cdot \boldsymbol{\sigma}, \quad (2)$$

one obtains the velocity operator

$$v^j = \frac{\hbar k^j}{m^*} + \frac{\partial \mathbf{h}_{\mathbf{k}} \cdot \boldsymbol{\sigma}}{\partial k^j}, \quad (3)$$

where $\boldsymbol{\sigma} \equiv (\sigma^x, \sigma^y, \sigma^z)$ is the Pauli matrix vector. In the case of the Rashba interaction, the spin-orbit field $\mathbf{h}_{\mathbf{k}}$ is given by

$$h_x = \alpha k_y, \quad h_y = -\alpha k_x. \quad (4)$$

We assume that the target impurity, located at \mathbf{r}_i , is represented by a scattering potential $U(\mathbf{r} - \mathbf{r}_i)$. The Green's functions in Eq. (1) have to be expanded in terms of this potential. Up to the second order in U , one obtains

$$\begin{aligned} G^{r/a}(\mathbf{r}, \mathbf{r}') &= G^{r/a(0)}(\mathbf{r}, \mathbf{r}') + \int ds^2 G^{r/a(0)}(\mathbf{r}, \mathbf{s}) U(\mathbf{s} - \mathbf{r}_i) \\ &\times G^{r/a(0)}(\mathbf{s}, \mathbf{r}') + \int ds^2 ds'^2 G^{r/a(0)}(\mathbf{r}, \mathbf{s}) U(\mathbf{s} - \mathbf{r}_i) \\ &\times G^{r/a(0)}(\mathbf{s}, \mathbf{s}') U(\mathbf{s}' - \mathbf{r}_i) G^{r/a(0)}(\mathbf{s}', \mathbf{r}'). \end{aligned} \quad (5)$$

The unperturbed functions $G^{r/a(0)}$ depend, nevertheless, on the scattering from background random impurities. The latter create the random potential $V_{sc}(\mathbf{r})$, which is assumed to be delta correlated, so that the pair correlator $\langle V_{sc}(\mathbf{r}) V_{sc}(\mathbf{r}') \rangle = \Gamma \delta(\mathbf{r} - \mathbf{r}') / \pi N_F$, where $\Gamma = 1/2\tau$ is expressed via the mean elastic scattering time τ . The delta correlation means that the corresponding impurity potential is the short-range one. In fact, the potential of the target impurity could be different from that of the random impurities. It might be a special sort

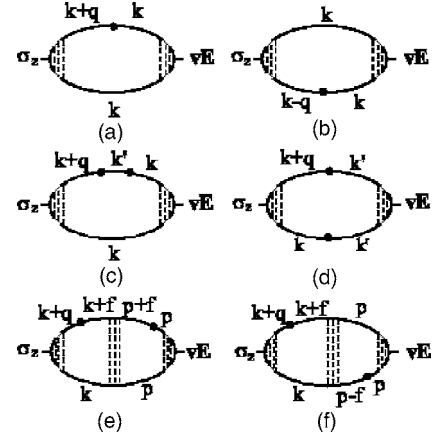


FIG. 1. Examples of diagrams for the spin density. Scattering of electrons by a target impurity is shown by the solid circles. Dashed lines denote the ladder series of particle scattering by the random potential. \mathbf{p}, \mathbf{k} , and \mathbf{k}' are the electron momenta.

of impurities added to the system. On the other hand, the target and the random impurities would be identical if one would try to employ the spin dipoles for the interpretation of spin accumulation near interfaces.

After the substitution of Eq. (5) into Eq. (1), one must calculate the background impurity configurational averages containing the products of several Green's functions $G^{(0)}$. Assuming that the semiclassical approximation $E_F \tau \gg 1$ is valid, the standard perturbation theory^{18,19} can be employed. Its building blocks are the so-called ladder perturbation series expressed in terms of the unperturbed average Green's functions

$$G_{\mathbf{k}}^{r/a} = \int d^2(\mathbf{r} - \mathbf{r}') e^{i\mathbf{k}(\mathbf{r} - \mathbf{r}')} \overline{G^{r/a(0)}(\mathbf{r}, \mathbf{r}')} \quad (6)$$

given by the 2×2 matrix,

$$G_{\mathbf{k}}^{r/a} = (E_F - E_{\mathbf{k}} - \mathbf{h}_{\mathbf{k}} \cdot \boldsymbol{\sigma} \pm i\Gamma)^{-1}, \quad (7)$$

where $E_{\mathbf{k}} = k^2 / (2m^*)$. When averaging the Green's function products within the ladder approximation, only pairs of retarded and advanced functions carrying close enough momenta should be chosen to become elements of the ladder series. After decoupling the mean products of Green's functions into the ladder series, the Fourier expansion of Eq. (1) can be represented by the diagrams shown in Fig. 1. In these diagrams, the diffusion ladder renormalizes both the left-hand and right-hand vertices. The renormalized left-hand vertex $\Sigma_z(\mathbf{q})$ is associated with the \mathbf{q} th Fourier component of the induced spin density, and the corresponding diffusion propagator enters with the wave vector \mathbf{q} . In its turn, the right-hand vertex $T(\mathbf{p})$ related to the homogeneous electric field is represented by the ladder at the zeroth wave vector. The corresponding physical process is the D'yakonov-Perel'²⁰ spin relaxation of a uniform spin distribution. This left-hand vertex alone contributed to the ballistic case result,¹⁴ while $\Sigma_z(\mathbf{q})$ has been taken unrenormalized due to large values of $\mathbf{q} \gg 1/(v_F \tau)$ in the ballistic regime. Figures 1(e) and 1(f) represent some diagrams where the diffu-

sion process separates two scattering events. As will be shown below, such diagrams give rise to small corrections to the spin density and can be neglected. Hence, the main contribution comes from the diagrams similar to those in Figs. 1(a)–1(d). The corresponding spin polarization has the form

$$S_z(\mathbf{q}) = \frac{1}{2\pi} \sum_{\mathbf{p}, \mathbf{k}} \text{Tr}[G_{\mathbf{p}\mathbf{k}}^a \Sigma_z(\mathbf{q}) G_{\mathbf{k}+\mathbf{q}, \mathbf{p}}^r T(\mathbf{p})]. \quad (8)$$

The functions $G_{\mathbf{k}'\mathbf{k}}^{r/a}$ are formally represented by the Fourier expansion of Eq. (5) with respect to \mathbf{r} and \mathbf{r}' , provided that the respective average values $G^{(0)}(\mathbf{r}, \mathbf{r}')$, instead of $G^{(0)}(\mathbf{r}, \mathbf{r}')$, are substituted. Evaluating the pair products of such functions in Eq. (8), one should take into account only the terms up to the second order with respect to the scattering potential U .

The vertices $\Sigma_z(\mathbf{q})$ and $T(\mathbf{p})$ can be easily calculated. As was discussed in Ref. 14, due to considerable cancellation of the diagrams which is known from literature on the spin-Hall effect, $T(\mathbf{p})$ acquires a quite simple form in a special case of the Rashba SOI. Namely,

$$T(\mathbf{p}) = \frac{e}{m} \mathbf{p} \cdot \mathbf{E}. \quad (9)$$

In its turn, $\Sigma_z(\mathbf{q})$ is expressed in terms of the diffusion propagator. Indeed, let us represent this vertex using a basis of four 2×2 matrices $\tau^0=1$ and $\tau^i=\sigma^i$, with $i=x, y, z$. Then, $\Sigma_z(\mathbf{q})$ can be written as

$$\Sigma_z(\mathbf{q}) = \sum_b D^{zb}(\mathbf{q}) \tau^b, \quad b=0, x, y, z, \quad (10)$$

where $D^{zb}(\mathbf{q})$ are the matrix elements of the diffusion propagator satisfying the spin-diffusion equation, as it was described in Ref. 6 and references therein. The nondiagonal element $D^{z0}(\mathbf{q})$ appears due to the spin-charge mixing and it is zero for SOI of a quite general form, including the Rashba interaction.^{21–24} Finally, from Eq. (8), using Eqs. (9) and (10), we express $S_z(\mathbf{q})$ in the form

$$S_z(\mathbf{q}) = \sum_{n=x, y, z} D^{zn}(\mathbf{q}) I^n(\mathbf{q}), \quad (11)$$

where

$$I^n(\mathbf{q}) = \frac{e}{2\pi m} \sum_{\mathbf{p}, \mathbf{k}} (\mathbf{p} \cdot \mathbf{E}) \text{Tr}[G_{\mathbf{p}\mathbf{k}}^a \sigma^n G_{\mathbf{k}+\mathbf{q}, \mathbf{p}}^r]. \quad (12)$$

The function $I^n(\mathbf{q})$ has a simple physical meaning. For $n=x, y, z$, it represents a source of spin-polarized particles emitting from the target impurity. Their further diffusion and spin relaxation result in the observable polarization. This source term feature is conceptually similar, though different in its context, to the original charge cloud consideration when SOI is not present and the Boltzmann equation is used to describe the subsequent background scattering.^{13,16} For $q \ll l^{-1} \ll k_F$, the source can be expanded in powers of q . Therefore, the wave-vector-independent terms represent the delta source located at \mathbf{r}_i , while the terms linear in q are associated with the gradient of the delta function. Below, we will keep only the constant and linear terms for each n th

component $I^n(\mathbf{q})$ and assume, for simplicity, the short-range scattering potential $U(\mathbf{r})$, so that its \mathbf{k} th Fourier transform is simply $U \exp(-i\mathbf{k} \cdot \mathbf{r}_i)$, where U is a constant. Further, $I^n(\mathbf{q})$ can be written as

$$I^n(\mathbf{q}) = I_1^n(\mathbf{q}) + I_2^n(\mathbf{q}), \quad (13)$$

where I_1 and I_2 are of the first and the second order with respect to the scattering potential U , respectively. Accordingly, I_1 and I_2 are represented by Figs. 1(a) and 1(b) and Figs. 1(c) and 1(d), respectively. Using Eq. (5) to express Green's functions $G_{\mathbf{k}'\mathbf{k}}^{r/a}$ in Eq. (12), we obtain

$$I_1^n(\mathbf{q}) = \frac{eU}{2\pi m} e^{i\mathbf{q} \cdot \mathbf{r}_i} \sum_{\mathbf{p}} (\mathbf{p} \cdot \mathbf{E}) \text{Tr}[G_{\mathbf{p}}^r G_{\mathbf{p}}^a (\sigma^n G_{\mathbf{p}+\mathbf{q}}^r + G_{\mathbf{p}-\mathbf{q}}^a \sigma^n)] \quad (14)$$

and

$$I_2^n(\mathbf{q}) = \frac{eU^2}{2\pi m} e^{i\mathbf{q} \cdot \mathbf{r}_i} \sum_{\mathbf{p}, \mathbf{k}} (\mathbf{p} \cdot \mathbf{E}) \text{Tr}[G_{\mathbf{p}}^r G_{\mathbf{p}}^a (G_{\mathbf{k}}^a \sigma^n G_{\mathbf{k}+\mathbf{q}}^r - \gamma \sigma^n G_{\mathbf{p}+\mathbf{q}}^r + \gamma G_{\mathbf{p}-\mathbf{q}}^a \sigma^n)], \quad (15)$$

where

$$\gamma = i \text{Im} \left(\sum_{\mathbf{k}} G_{\mathbf{k}}^a \right) = i\pi N_F. \quad (16)$$

In our following consideration, we let the x -axis be parallel with the electric field and the z -axis be perpendicular to the 2DEG. The system Hamiltonian is symmetric under a symmetry operation combining a reflection from the plane perpendicular to the y -axis, that is, $p_y \rightarrow -p_y$, and a unitary transformation $\sigma^i \rightarrow \sigma_y \sigma^i \sigma_y$. Applying this transformation to Eq. (12), one can easily see that $I^x(q_x, q_y) = -I^x(q_x, -q_y)$, $I^z(q_x, q_y) = -I^z(q_x, -q_y)$, and $I^y(q_x, q_y) = I^y(q_x, -q_y)$. Making use of another symmetry operation $p_x \rightarrow -p_x$, $p_y \rightarrow -p_y$, and $\sigma^i \rightarrow \sigma_z \sigma^i \sigma_z$, we obtain $I^x(q_x, q_y) = I^x(-q_x, -q_y)$, $I^z(q_x, q_y) = -I^z(-q_x, -q_y)$, and $I^y(q_x, q_y) = I^y(-q_x, -q_y)$. From these relations, it is easy to see that the expansion of I^z into a power series starts from linear in \mathbf{q} terms, while the leading term in I^y is constant and the next one is quadratic in q . Because of this reason, only the constant will be taken into account in I^y . The expansion of I^x starts from $q_x q_y$, and this source component will be neglected.

The calculation of I_1 and I_2 given by Eqs. (14) and (15) is based on the standard linearization near the Fermi level, thus ignoring band effects giving rise to small corrections $\sim h_{k_F}/E_F$ and Γ/E_F . Further, the diffusion approximation is valid at $q \ll 1/l$. At the same time, the characteristic length scale is determined by the spin-relaxation length l_{so} , which is the distance a particle diffuses during the D'yakonov-Perel' spin-relaxation time $\tau_{so} = 4(h_{k_F}^2 \tau)^{-1}$. The corresponding diffusion length $l_{so} = \sqrt{D\tau_{so}}$, where $D = v_F^2 \tau / 2$ is the diffusion constant. Hence, $l_{so} = v_F / h_{k_F}$. Taking $q \sim 1/l_{so}$, one finds that the diffusion approximation is valid if $h_{k_F} / \Gamma \ll 1$. Therefore, within this approximation, we will retain only the leading powers of $h_{k_F} / \Gamma \ll 1$. In such a way, direct calculation of I_1^n

with Green's functions and SOI given by Eqs. (7) and (4), respectively, shows that both I_1^y and I_1^z are small by a factor of Γ/E_F . For example, using the relation

$$(G_{\mathbf{k}}^{r(a)})^2 = -\frac{\partial}{\partial E_F} G_{\mathbf{k}}^{ra}, \quad (17)$$

which follows from Eq. (7), evaluating I_1^y at $q=0$, one can represent the corresponding sum in Eq. (14) as

$$-\frac{\partial}{\partial E_F} \sum_{\mathbf{p}} p_x \text{Tr}[G_{\mathbf{p}}^r G_{\mathbf{p}}^a \sigma^y] = -\frac{\partial}{\partial E_F} \left(\frac{2\pi}{\Gamma} N_F m^* \frac{\partial h_{\mathbf{p}}^y}{\partial p_x} \right). \quad (18)$$

In the case of the Rashba SOI with the constant coupling strength α and energy-independent parameters Γ, m^* , and N_F , the sum (18) is equal to 0. Otherwise, it is finite, but small due to the smooth energy dependence of these parameters. A similar analysis, although not so straightforward, can be applied to I_1^z , which is linear in q . The smallness of I_1^z can also be seen from Ref. 14, where the contribution to the spin density linear in U was associated with fast Friedel oscillations. It is clear that their Fourier transform will be small in the range of $q \ll k_F^{-1}$.

At the same time, I_2^y and I_2^z are not zero. They are given by

$$\begin{aligned} I^y &= v_d N_F m^* \alpha h_{k_F}^2 \frac{\Gamma'}{\Gamma^3}, \\ I^z &= -i q_y v_d N_F h_{k_F}^2 \frac{\Gamma'}{2\Gamma^3}, \\ I^x &= 0, \end{aligned} \quad (19)$$

where $\Gamma' = \pi N_F U^2$ and $v_d = eE\tau/m^*$ is the electron drift velocity. If the target impurity is represented by one of the random scatterers, we get $\Gamma' = \Gamma/n_i$, where n_i is the density of impurities.

In the above calculation, we did not take into account the diagrams shown in Figs. 1(e) and 1(f) and those similar to them. It can be easily seen that such diagrams contain I_1^y as a factor. For example, the sum of the diagrams in Figs. 1(e) and 1(f) contains as a multiplier the sum of the diagrams shown in Figs. 1(a) and 1(b). Therefore, such diagrams are small by the same reason as I_1^y are, at least, in the most important range of $f \ll l^{-1}$. Particularly, in this range of small f , the diffusion propagator between the two scattering events in Figs. 1(e) and 1(f) becomes large.

Now, one can combine the source I^n with the diffusion propagator to find from Eq. (11) the shape of the spin cloud around a single scatterer. Taking into account Eq. (19), Eq. (11) is transformed into

$$S_z(\mathbf{q}) = -v_d N_F h_{k_F}^2 \frac{\Gamma'}{2\Gamma^3} [i q_y D^{zz}(\mathbf{q}) - 2m^* \alpha D^{zy}(\mathbf{q})]. \quad (20)$$

The matrix elements $D^{ij}(\mathbf{q})$ satisfy the spin-diffusion equation^{6,25}

$$\sum_l \left(-\delta^l D q^2 - \Gamma^{il} + i \sum_m R^{ilm} q_m \right) D^{lj}(\mathbf{q}) = -2\Gamma \delta_{ij}, \quad (21)$$

where the matrix Γ^{il} determining the D'yakonov-Perel' spin-relaxation rates is given by

$$\Gamma^{il} = 4\tau \langle \delta^i h_{k_F}^2 - h_{k_F}^i h_{k_F}^l \rangle, \quad (22)$$

with the angular brackets denoting averaging over the Fermi surface. In the case of the Rashba SOI [Eq. (4)] one gets $\Gamma^{zz} = 4\tau h_{k_F}^2$ and $\Gamma^{xx} = \Gamma^{yy} = 2\tau h_{k_F}^2$. The last term in the left-hand side of Eq. (21) is associated with spin precession in the SOI field. It has the form

$$R^{ilm} = 4\tau \sum_p \varepsilon^{ilp} \langle h_{k_F}^p v_F^m \rangle. \quad (23)$$

For the Rashba SOI, the nonzero components are

$$i \sum_m R^{izm} q_m = -i \sum_m R^{zim} q_m = 4i D m^* \alpha q_i. \quad (24)$$

We ignored in Eq. (21) a small term which gives rise to the spin-charge mixing.^{6,23,24} This mixing is already taken into account in the source term because I^n for $n=x, y, z$ describes the source of the *spin polarization* in response to the *electric* field. From Eqs. (21)–(24), one finds

$$\begin{aligned} D^{zz} &= \frac{1}{2h_{k_F}^2 \tau^2} \frac{\tilde{q}^2 + 1}{(\tilde{q}^2 + 2)(\tilde{q}^2 + 1) - 4\tilde{q}^2}, \\ -D^{zy} = D^{yz} &= \frac{1}{2h_{k_F}^2 \tau^2} \frac{2i\tilde{q}_y}{(\tilde{q}^2 + 2)(\tilde{q}^2 + 1) - 4\tilde{q}^2}, \\ D^{yy} &= \frac{1}{2h_{k_F}^2 \tau^2} \frac{\tilde{q}^2 + 2}{(\tilde{q}^2 + 2)(\tilde{q}^2 + 1) - 4\tilde{q}^2}, \end{aligned} \quad (25)$$

where $2\tilde{q} = l_{\text{so}} q$ denotes the dimensionless wave vector. Substituting Eq. (25) into Eq. (20), we finally find

$$S_z = -2i v_d \frac{m^* \alpha}{\hbar} N_F \frac{\Gamma'}{\Gamma} \frac{\tilde{q}_y (\tilde{q}^2 + 3)}{(\tilde{q}^2 + 2)(\tilde{q}^2 + 1) - 4\tilde{q}^2} \quad (26)$$

and

$$S_y = 2v_d \frac{m^* \alpha}{\hbar} N_F \frac{\Gamma'}{\Gamma} \frac{(3\tilde{q}^2 + 2)}{(\tilde{q}^2 + 2)(\tilde{q}^2 + 1) - 4\tilde{q}^2}. \quad (27)$$

To restore the conventional units, we added \hbar into Eqs. (26) and (27). The z -component of the spin density in real space is shown in Fig. 2. According to expectations, it has the shape of a dipole oriented perpendicular to the electric field. Its spatial behavior is determined by the single parameter l_{so} , which gives the range of exponential decay of the spin polarization with increasing distance from an impurity. The S_y component averaged over impurity positions gives the uniform bulk polarization. It is interesting to note that when the target impurities are identical to the background ones ($\Gamma' = \Gamma$), the so obtained uniform polarization $S_y|_{q \rightarrow 0}$ coincides with the electric spin orientation¹⁵ $S_y = 2v_d m^* \alpha N_F / \hbar$.

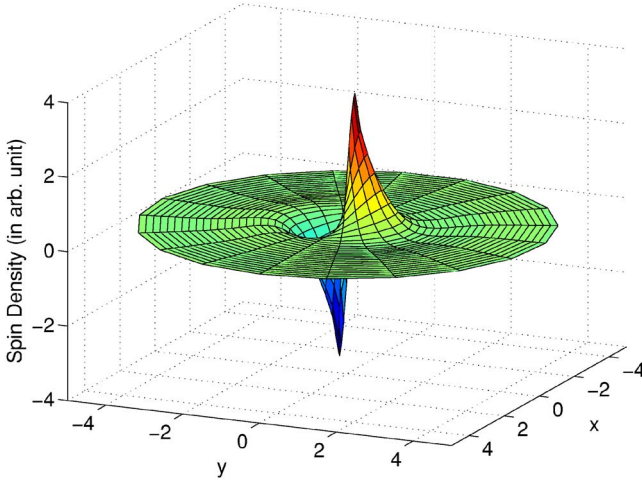


FIG. 2. (Color online) Spatial distribution of S_z component of the spin density around a single scatterer. The unit of length $=l_{so}$.

III. SPIN ACCUMULATION IN A SEMI-INFINITE SYSTEM

In this section, we will consider a semi-infinite electron gas $y > 0$ bounded at $y=0$ by a boundary parallel to the electric field. Our goal is to calculate a combined effect of spin clouds from random impurities. It is important to note that the summation of spin dipoles from many scatterers does not result in a magnetic potential gradient in the bulk of the sample. This is principally different from the Landauer charge dipoles, which are associated with the macroscopic electric field. The origin of such a distinction can be immediately seen from Eq. (26). The magnetic potential, as it was defined in Sec. I, is proportional to S_z . By taking its gradient, one gets $q_y S_z$. After averaging over impurity positions $q \rightarrow 0$, $q_y S_z \rightarrow 0$. It happens due to spin relaxation, which provides at $q=0$ a finite value of the denominator in Eq. (26). At the same time, in the case of the charge cloud, the denominator of the particle diffusion propagator is proportional to q^2 . Hence, the corresponding gradient of the electrochemical potential (electric field) is finite at $q=0$. Although the bulk magnetic potential is zero, one cannot expect that it will also be zero near an interface. In order to calculate the spin polarization near the boundary, Eq. (21), with $\mathbf{q} = -i\nabla$ and $2\Gamma\delta(\mathbf{r})\delta_{ij}$ in the right-hand side, has to be solved using appropriate boundary conditions. With the so obtained $D^{ij}(\mathbf{r})$, the resultant spin density induced by impurities placed at points \mathbf{r}_i is given by Eq. (11),

$$S_j(\mathbf{r}) = \sum_{n=x,y,z} \int d^2r' D^{jn}(\mathbf{r}-\mathbf{r}') I_{tot}^n(\mathbf{r}'), \quad (28)$$

where the source term is obtained by the inverse Fourier transform of Eq. (19):

$$I_{tot}^y(\mathbf{r}) = v_d N_F m^* \alpha h_{k_F}^2 \frac{1}{\Gamma^2} \sum_i \delta(\mathbf{r}-\mathbf{r}_i),$$

$$I_{tot}^z(\mathbf{r}) = -v_d N_F h_{k_F}^2 \frac{1}{2\Gamma^2} \sum_i \frac{\partial}{\partial y} \delta(\mathbf{r}-\mathbf{r}_i),$$

$$I_{tot}^x(\mathbf{r}) = 0. \quad (29)$$

where the relation $\Gamma' = \Gamma/n_i$ is used because we assumed that the target impurities are identical to the random ones. The macroscopic polarization is obtained by averaging of Eqs. (28) and (29) over impurity positions. After averaging over x_i and the semi-infinite region $y_i > 0$, the spin-polarization source (29) transforms to $I_{av}^n(y)$:

$$I_{av}^y(y) = v_d N_F m^* \alpha h_{k_F}^2 \frac{1}{\Gamma^2},$$

$$I_{av}^z(y) = -v_d N_F h_{k_F}^2 \delta(y-0^+) \frac{1}{2\Gamma^2}. \quad (30)$$

It follows from Eq. (28) that the corresponding mean value of the spin polarization, $\mathbf{S}_{av}(y)$, satisfies the diffusion equation (21) with the source $2\Gamma I_{av}^n(y)$ in its right-hand side. The so obtained diffusion equation, however, is not complete. One should take into account that the boundary itself can create the interface spin polarization. Most easily, it can be done in the framework of the Boltzmann approach. In terms of the Boltzmann function, the spin density is defined as $\mathbf{S}_{av}(y) = \sum_{\mathbf{k}} \mathbf{g}_{\mathbf{k}}$, and the charge density as $\sum_{\mathbf{k}} g_{\mathbf{k}}$. The equation for the Boltzmann function can be written in the form (see, e.g., Ref. 26)

$$v_g \nabla_y \mathbf{g}_{\mathbf{k}} + 2(\mathbf{g}_{\mathbf{k}} \times \mathbf{h}_{\mathbf{k}}) + eE_x \frac{\partial \mathbf{g}_{\mathbf{k}}^{(0)}}{\partial k_x} = \frac{1}{\tau} [\mathbf{S}_E(y) - \mathbf{g}_{\mathbf{k}}], \quad (31)$$

where $\mathbf{S}_E(y) = \delta(E-E_F) \mathbf{S}_{av}(y) / N_F$ and $\mathbf{g}_{\mathbf{k}}^{(0)} = -\mathbf{h}_{\mathbf{k}} \delta(E-E_F)$ is the equilibrium Boltzmann function. The terms proportional to the charge component of the Boltzmann function have been omitted in Eq. (31) due to the system local electroneutrality, at least in the scale of the mean free path, which is the smallest characteristic scale of $\mathbf{g}_{\mathbf{k}}$ spatial variations. The scattering part of Eq. (31) is written in the simple relaxation time approximation. Such a scattering term follows²⁶ from the Keldysh formalism assuming isotropic scattering from impurities, as has been adopted in this work. For angular dependent scattering, however, a structure of the scattering term is more complicated.²⁷

The spin-polarization source associated with the boundary is given by a direct action of the electric field, without taking into account secondary scattering from impurities. Hence, the term with $\mathbf{S}_{av}(y)$ in the right-hand side of Eq. (31) can be ignored. Also, the boundary independent bulk part of $\mathbf{g}_{\mathbf{k}}$ has to be subtracted from the general solution of Eq. (31). The so obtained interface Boltzmann function will be denoted as $\mathbf{g}_{\mathbf{k}if}$. The corresponding spin density is $\mathbf{S}_{if}(y) = \sum_{\mathbf{k}} \mathbf{g}_{\mathbf{k}if}$. In order to calculate $\mathbf{g}_{\mathbf{k}if}$, Eq. (31) has to be supplemented with the boundary condition. For a hard wall specularly reflecting boundary, the condition is simply

$$\mathbf{g}_{k_x, k_y}|_{z=0} = \mathbf{g}_{k_x, -k_y}|_{z=0}. \quad (32)$$

This condition means that the spin orientation does not change after specular reflection from the interface. The solution of Eq. (31) satisfying Eq. (32) can be easily found. As a result, up to $o(\alpha^2)$, we obtain

$$\begin{aligned} S_{\text{if}}^y(y) &= S_{\text{if}}^x(y) = 0, \\ S_{\text{if}}^z(y) &= 8v_d \alpha^2 \pi m^* \sum_{k_y > 0} k_y \delta(E_{\mathbf{k}} - E_F) e^{-y(m^*/\hbar k_y \tau)}. \end{aligned} \quad (33)$$

Within the diffusion approximation, the second of these equations represents a delta source of the spin polarization with intensity

$$\frac{1}{\tau} \int_0^\infty dy S_{\text{if}}^z(y) = v_d N_F \hbar k_F^2 \frac{1}{\Gamma}. \quad (34)$$

This source is exactly of the same magnitude, but opposite in sign to the spin polarization emerging from impurities, which is represented by the integral of $2\Gamma I_{\text{av}}^z(y)$, with $I_{\text{av}}^z(y)$ given by Eq. (30). Taking into account that both sources are located at the interface, so that they cancel each other out, one sees that only the y -component of the source originating from impurity scattering retains in the diffusion equation which acquires the form

$$\begin{aligned} \frac{\partial^2 S_{\text{av}}^z}{\partial y^2} - 4m^* \alpha \frac{\partial S_{\text{av}}^y}{\partial y} - 8m^{*2} \alpha^2 S_{\text{av}}^z &= 0, \\ \frac{\partial^2 S_{\text{av}}^y}{\partial y^2} + 4m^* \alpha \frac{\partial S_{\text{av}}^z}{\partial y} - 4m^{*2} \alpha^2 S_{\text{av}}^y &= -\frac{2\Gamma}{D} I_{\text{av}}^y. \end{aligned} \quad (35)$$

The bulk solutions of this equation are $S_{\text{av}}^z=0$ and $S_{\text{av}}^y \equiv S_b = 2\tau e N_F \alpha$, which coincide with the polarization obtained from Eqs. (26) and (27) at $q \rightarrow 0$.

In order to calculate the spin polarization near the interface, we employ the hard wall boundary conditions^{6,8,9} for Eq. (35). Such boundary conditions can be easily obtained from Eq. (31) by performing its summation over \mathbf{k} and integrating from $y=0$ to some point y_0 , placed at a distance much larger than l but still small compared to l_{so} . A simple analysis of Eq. (31) shows that up to $o(\alpha^2)$, the sum over \mathbf{k} of the vector product in the left-hand side of Eq. (31) can be neglected, while the right-hand side and the term containing the electric field turn to zero identically. As a result, we get

$$\frac{1}{m^*} \sum_{\mathbf{k}} k_y \mathbf{g}_{k_x, k_y}|_{y=y_0} = \frac{1}{m^*} \sum_{\mathbf{k}} k_y \mathbf{g}_{k_x, k_y}|_{y=0}. \quad (36)$$

According to Eq. (32), the above sum is zero at $y=0$. Hence, it is also zero at $y=y_0$. The latter sum coincides with the spin current within its conventional definition,²⁶ where a contribution associated with the charge density due to the second term of the velocity operator (3) is ignored in an electroneutral system. Using the gradient expansion of Eq. (31), this current can easily be expressed²⁶ through $S_{\text{av}}^j|_{y=0}$, its y -derivative, and the last term in the left-hand side of Eq. (31). In this way, one arrives at the boundary conditions from Refs. 6, 8, and 9. We generalize these conditions by adding pos-

sible effects of the surface spin relaxation (see also Ref. 10). These additional terms are characterized by the two phenomenological parameters ρ_y and ρ_z . Finally, we obtain

$$\begin{aligned} -D \left. \frac{\partial S_{\text{av}}^z(y)}{\partial y} \right|_{y=0} + 2Dm^* \alpha [S_{\text{av}}^y(0) - S_b] &= -\rho_z S_{\text{av}}^z(0), \\ -D \left. \frac{\partial S_{\text{av}}^y(y)}{\partial y} \right|_{y=0} - 2Dm^* \alpha S_{\text{av}}^z(0) &= -\rho_y S_{\text{av}}^y(0). \end{aligned} \quad (37)$$

One can easily see from Eqs. (35) and (37) that at $\rho_{x/y}=0$, the homogeneous bulk solutions $S_{\text{av}}^z=0$ and $S_{\text{av}}^y=S_b$ turn out to be the solutions of the diffusion equation everywhere at $y>0$. Therefore, in this particular case, the z -components of spin clouds from many impurities completely cancel each other out and there is no spin accumulation near the interface. This result, as well as boundary conditions (37) for the hard wall case, agrees with Refs. 6–9. A different result has been obtained, however, in Ref. 10, where a method similar to Ref. 8 has been employed. Such a distinction requires a special analysis outside the goals of the present work.

When $\rho_i \neq 0$, the out-of-plane component of the spin density is not zero. In the case of weak surface relaxation, $\rho_i \ll D/l_{\text{so}}$, one obtains the following from Eqs. (37) and (35):

$$S_{\text{av}}^z(0) = 0.35 \rho_y \tau e E \frac{1}{2\pi \hbar D}, \quad (38)$$

where we inserted \hbar to restore conventional units. It is interesting to note that in such a regime of small enough ρ_i , the surface polarization does not depend on the spin-orbit constant.

IV. SPIN-HALL RESISTANCE AND ENERGY DISSIPATION

As it was defined in the Introduction, the interface spin-Hall resistance is given by

$$R_{\text{SH}} = \frac{S_{\text{av}}^z(0)}{N_F j}, \quad (39)$$

where j is the dc density, $j = \sigma E$, with the Drude conductivity $\sigma = ne^2 \tau / m^*$. The so defined spin-Hall resistance is closely related to the additional energy dissipation which takes place due to spin accumulation and relaxation near the interfaces of a sample. Indeed, as was shown in Ref. 6, the spin accumulation is associated with a correction to the electric conductivity of the dc flowing in the x -direction. For the Rashba SOI, the correction to the current density has the form

$$\Delta j(y) = -\frac{e}{4m^*} \frac{\alpha^2 k_F^2}{\Gamma^2} \frac{\partial S_{\text{av}}^z}{\partial y}. \quad (40)$$

This expression is finite within the distance of $\sim l_{\text{so}}$ from the interface. After integration over y , one obtains a correction to the electric current,

$$\Delta I = \frac{e}{4m^*} \frac{\alpha^2 k_F^2}{\Gamma^2} S_{\text{av}}^z(0). \quad (41)$$

The corresponding interface energy dissipation (per unit of the interface length) can be expressed from Eqs. (39) and (41) as

$$\Delta W = \Delta IE = \frac{m^*}{e\hbar^3} \alpha^2 \tau R_{\text{SH}} j^2. \quad (42)$$

In its turn, R_{SH} can be determined from Eq. (38). It can be easily seen that $\Delta W > 0$ if $\rho_y > 0$.

V. RESULTS AND DISCUSSION

Summarizing the above results within the drift diffusion theory, we found out that the intrinsic spin-Hall effect induces in 2DEG a nonequilibrium spin density around a spin-independent isotropic elastic scatterer. The z -component of this density has the shape of a dipole directed perpendicular to the external electric field, while the polarization parallel to 2DEG is isotropic. Due to the D'yakonov-Perel' spin relaxation, the spin density decays exponentially at a distance larger than the spin-orbit precession length. It is noteworthy that such a cloud exists even in the case of the Rashba spin-orbit interaction when the macroscopic spin current is absent. We also calculated the macroscopic spin density near an interface by taking the sum of clouds due to many scatterers and independently averaging over their positions. Surprisingly, in the case of the hard wall boundary, the so calculated spin polarization exactly coincides with that found from the drift diffusion or Boltzmann equations.⁶⁻⁹ In this case, the

out-of-plane component of the spin polarization is zero, while the parallel polarization is a constant determined by the electric spin orientation.¹⁵ Besides the hard wall boundary, we also considered a more general boundary condition containing the interface spin relaxation, or the spin leaking term. For such a general case, $S^z \neq 0$. This polarization can be associated with the local magnetic potential because the system attains its local equilibrium within the S^z spatial variation scale, which is much larger than l . The magnetic potential, in its turn, is related to the dc electric current density via the interface spin-Hall resistance. The latter was shown to determine the additional energy dissipation due to the relaxation of the spin polarization near the interface.

Besides conventional semiconductor quantum wells, the results of this work can be applied to metal adsorbate systems with strong Rashba-type spin splitting in the surface states.²⁸ In this case, the spin cloud can be measured by a scanning-tunneling microscope with a magnetic tip.

ACKNOWLEDGMENTS

This work was supported by RFBR Grant No. 060216699, NSC 95-2112-M-009-004, the MOE-ATU Grant, and NCTS Taiwan. We are grateful to the Centre for Advanced Study in Oslo for their hospitality.

-
- ¹H.-A. Engel, E. I. Rashba, and B. I. Halperin, cond-mat/0603306 (unpublished).
²S. Murakami, N. Nagaosa, and S.-C. Zhang, *Science* **301**, 1348 (2003); J. Sinova, D. Culcer, Q. Niu, N. A. Sinitsyn, T. Jungwirth, and A. H. MacDonald, *Phys. Rev. Lett.* **92**, 126603 (2004); D. Culcer, J. Sinova, N. A. Sinitsyn, T. Jungwirth, A. H. MacDonald, and Q. Niu, *ibid.* **93**, 046602 (2004).
³M. I. Dyakonov and V. I. Perel, *Phys. Lett.* **35A**, 459 (1971); J. E. Hirsch, *Phys. Rev. Lett.* **83**, 1834 (1999).
⁴Y. K. Kato, R. C. Myers, A. C. Gossard, and D. D. Awschalom, *Science* **306**, 1910 (2004).
⁵J. Wunderlich, B. Kaestner, J. Sinova, and T. Jungwirth, *Phys. Rev. Lett.* **94**, 047204 (2005).
⁶A. G. Mal'shukov, L. Y. Wang, C. S. Chu, and K. A. Chao, *Phys. Rev. Lett.* **95**, 146601 (2005).
⁷R. Raimondi, C. Gorini, P. Schwab, and M. Dzierzawa, *Phys. Rev. B* **74**, 035340 (2006).
⁸O. Bleibaum, *Phys. Rev. B* **74**, 113309 (2006).
⁹Y. Tserkovnyak, B. I. Halperin, A. A. Kovalev, and A. Brataas, cond-mat/0610190 (unpublished).
¹⁰V. M. Galitski, A. A. Burkov, and S. D. Sarma, *Phys. Rev. B* **74**, 115331 (2006).
¹¹İ. Adagideli and G. E. W. Bauer, *Phys. Rev. Lett.* **95**, 256602 (2005).
¹²B. K. Nikolić, S. Souma, L. P. Zârbo, and J. Sinova, *Phys. Rev. Lett.* **95**, 046601 (2005); Q. Wang, L. Sheng, and C. S. Ting, cond-mat/0505576 (unpublished).
¹³R. Landauer, *IBM J. Res. Dev.* **1**, 223 (1957); *Philos. Mag.* **21**, 863 (1970).
¹⁴A. G. Mal'shukov and C. S. Chu, *Phys. Rev. Lett.* **97**, 076601 (2006).
¹⁵V. M. Edelstein, *Solid State Commun.* **73**, 233 (1990); J. I. Inoue, G. E. W. Bauer, and L. W. Molenkamp, *Phys. Rev. B* **67**, 033104 (2003).
¹⁶R. S. Sorbello and C. S. Chu, *IBM J. Res. Dev.* **32**, 58 (1988); C. S. Chu and R. S. Sorbello, *Phys. Rev. B* **38**, 7260 (1988).
¹⁷W. Zwerger, L. Bönig, and K. Schonhammer, *Phys. Rev. B* **43**, 6434 (1991).
¹⁸A. A. Abrikosov, L. P. Gor'kov, and I. E. Dzyaloshinskii, *Methods of Quantum Field Theory in Statistical Physics* (Dover, New York, 1975).
¹⁹B. L. Altshuler and A. G. Aronov, in *Electron-Electron Interactions in Disordered Systems*, edited by A. L. Efros and M. Pollak (North-Holland, Amsterdam, 1985).
²⁰M. I. D'yakonov and V. I. Perel', *Sov. Phys. JETP* **33**, 1053 (1971) [*Zh. Eksp. Teor. Fiz.* **60**, 1954 (1971)].
²¹A. G. Mal'shukov and K. A. Chao, *Phys. Rev. B* **71**, 121308(R) (2005).
²²J. I. Inoue, G. E. W. Bauer, and L. W. Molenkamp, *Phys. Rev. B* **70**, 041303(R) (2004).
²³E. G. Mishchenko, A. V. Shytov, and B. I. Halperin, *Phys. Rev. Lett.* **93**, 226602 (2004).
²⁴A. A. Burkov, A. S. Nunez, and A. H. MacDonald, *Phys. Rev. B* **70**, 155308 (2004).
²⁵A. G. Mal'shukov and K. A. Chao, *Phys. Rev. B* **61**, R2413 (2000).
²⁶C. S. Tang, A. G. Mal'shukov, and K. A. Chao, *Phys. Rev. B* **71**, 195314 (2005).
²⁷A. V. Shytov, E. G. Mishchenko, H.-A. Engel, and B. I. Halperin, *Phys. Rev. B* **73**, 075316 (2006); N. A. Sinitsyn, A. H. MacDonald, T. Jungwirth, V. K. Dugaev, and J. Sinova, cond-mat/0608682 (unpublished).
²⁸C. R. Ast, D. Pacile, M. Falub, L. Moreschini, M. Papagno, G. Wittich, P. Wahl, R. Vogelgesang, M. Grioni, and K. Kern, cond-mat/0509509 (unpublished).